A New Design Methodology for the Ultimate Capacity of Slender Prestressed Concrete Columns

Ahmed B. Shuraim, Ph.D.
Associate Professor of Civil Engineering
Civil Engineering Department
College of Engineering
King Saud University
Riyadh, Saudi Arabia

Antoine E. Naaman, Ph.D., FPCI
Professor of Civil Engineering
Civil and Environmental Engineering Department
College of Engineering
University of Michigan
Ann Arbor, Michigan

This paper presents a new method for computing the flexural rigidity, EI, of prestressed concrete columns at their ultimate capacity. Flexural rigidity is needed to evaluate the critical buckling load which is used in the magnification formula. The proposed methodology for computing EI is based on two fundamental relationships: (1) the moment versus curvature relationship at a given load eccentricity, and (2) buckling under the assumption of pure concentric load. The proposed EI model was used with the moment magnification formula to obtain moment versus axial load interaction diagrams for a number of slender prestressed concrete columns. The diagrams were compared with those obtained from a finite element analysis and very good agreement was observed. Also good agreement was observed with available experimental test results. Comparisons with current code formulations and PCI recommendations are made, and a new procedure is proposed. Several numerical design examples, illustrating the new method, are provided.

Slenderness effects and possible buckling in prestressed concrete columns have challenged the minds of researchers for more than four decades. Several theories and some formulations have been proposed but none have been completely satisfactory. Nonetheless, over the years, the performance of prestressed concrete columns in actual structures has been satisfactory and the demand for such members will definitely increase in the future.

Extensive investigations on prestressed concrete columns have been carried out by many researchers; included among these researchers are Lin and Itaya (1957),[1] Zia and Moreadith (1966),[2] Brown and Hall (1966),[3] Kabaila and Hall (1966),[4] Aroni (1967, 1968),[5,6] Nathan (1972 to 1985),[7,8,9,10] Yuan (1987),[11] Issa and Yuan (1989),[12] the PCI Committee on Prestressed Concrete Columns (1988),[13] Shuraim and Naaman (1989),[14] and Shuraim (1990).[15]

While several of the above studies involved experimental work, most

investigators tried to develop accurate models capable of predicting the behavior as well as the ultimate strength of slender prestressed concrete columns. In addition, some authors derived simple design recommendations for practical implementation.

For the past three decades, the ACI Building Code (ACI 318)[16] has adopted the magnification formula for the design of slender concrete columns. The main function of the formula may be explained with reference to Fig. 1, which shows a simply supported column, subjected to equal eccentric axial loads, P, at its ends.

As the column deflects under such a loading, its midspan section is subject to an additional moment of $P\Delta_{mid}$, where Δ_{mid} is the deflection at midspan. Thus, the total moment for which the column should be designed for is $M_{mid} = M_{end} + P\Delta_{mid}$. The magnification formula attempts to estimate the total moment without evaluating Δ_{mid} explicitly.

In practice, the magnification factor should neither be underestimated, thus risking an unsafe structure, nor overestimated, thus leading to an uneconomical design. The formula was originally derived for simply supported columns subject to axial compressive load and end moments assuming linear elastic materials. It is usually expressed as follows:

$$M_{mid} = \frac{M_{end}}{1 - \dfrac{P}{P_{cr}}} \qquad (1)$$

in which

M_{end} = moment at the end of the column (that is, $M = Pe$)
P = axial load at the end of the column
P_{cr} = critical buckling load when the column is under concentric axial compression
M_{mid} = total moment at midspan (see Fig. 1)

The Euler critical buckling load is given by:

$$P_{cr} = \frac{\pi^2 EI}{L^2} \qquad (2)$$

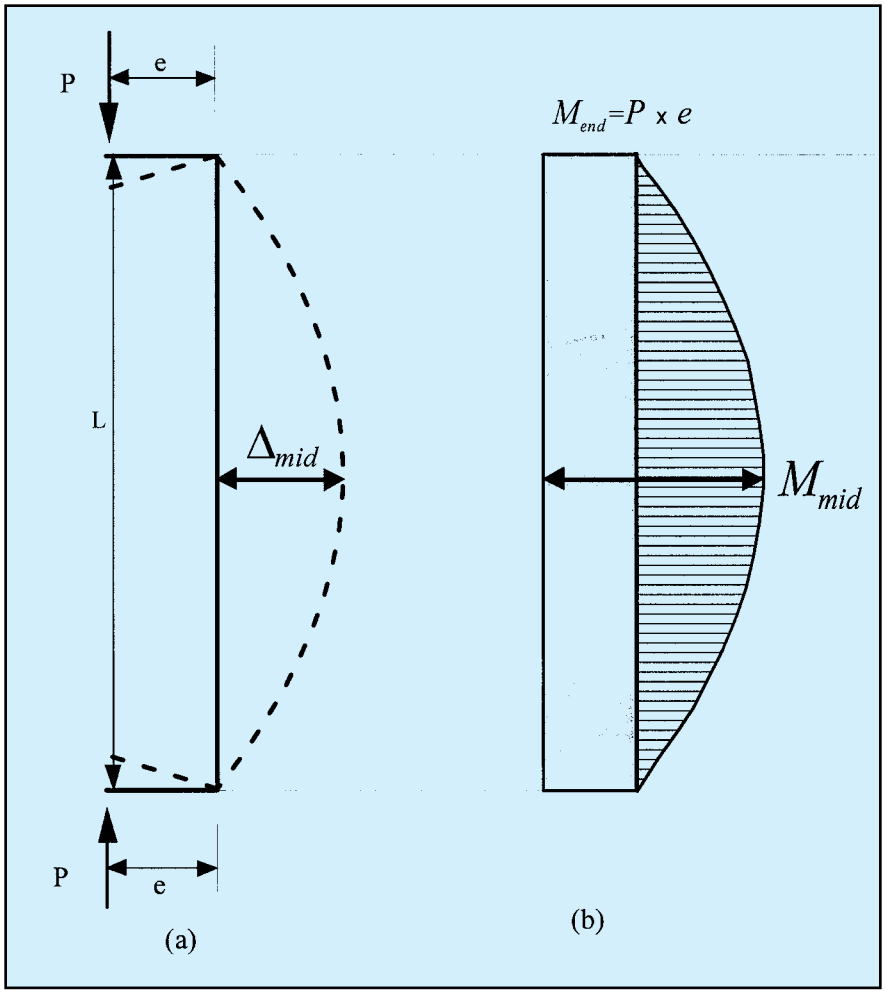

Fig. 1. Model of slender column under equal end moments and axial load: (a) Deformed shape; (b) Magnified moment at midspan.

where

L = length of the column
I = moment of inertia of the column cross section
E = modulus of elasticity

When Eqs. (1) and (2) were adopted for concrete columns in which the materials are essentially nonlinear and inelastic to a large degree, modifications were introduced regarding the flexural rigidity EI. Consequently, the validity of the equations depends on how accurately the flexural rigidity can be estimated.

This paper describes the main results of an investigation to evaluate the effective flexural rigidity, EI, used in Eq. (2) to calculate the buckling load for prestressed concrete (PC) columns and hence, through Eq. (1), to estimate the load carrying capacity of slender PC columns. The proposed methodology for computing EI was formulated based on two fundamental relationships:

The first relates moment to curvature at a given load eccentricity and the second is based on the concept of buckling under the assumption of pure concentric load.

The proposed methodology was developed following an extensive analytical evaluation of the behavior of numerous PC columns through a finite element analysis.[14,15] The effect of many parameters such as nonlinear properties of the component materials, cracking, slenderness ratio, irregular section geometry, level of effective prestress, prestressing reinforcement ratio, and different boundary conditions were considered.

A computer program was written to carry out the simplified calculations, verify the accuracy and fine-tune the calibration of the proposed design method vis-à-vis the finite element analysis. Also, the accuracy of

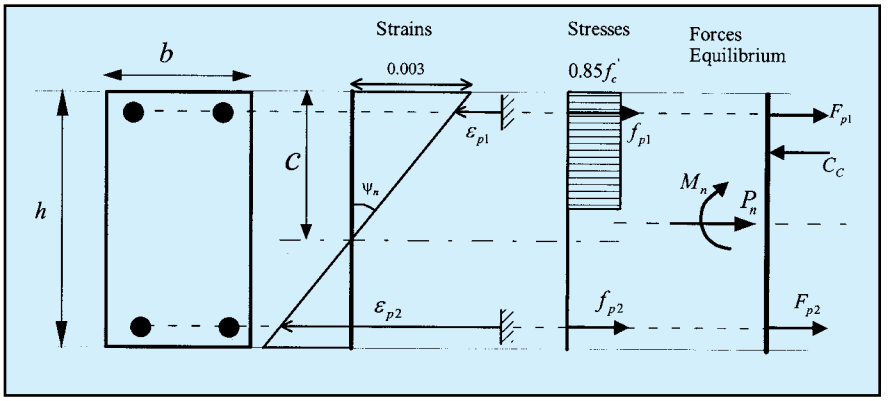

Fig. 2. Sectional analysis of prestressed concrete column based on compatibility and equilibrium requirements.

the model was verified by comparing predicted results with experimental data from the technical literature. The program was then used to evaluate a wide range of parameters.

BACKGROUND ON FLEXURAL RIGIDITY (*EI*)

This section presents the ACI Code provisions for determining flexural rigidity and the PCI recommendations for evaluating slenderness effects of columns.

Current ACI 318 Equations for *EI*

To account for the influence of cracking, softening and creep of concrete in addition to the yield of reinforcement, in lieu of a more accurate analysis, the ACI Code recommends the use of the following simple design equations for calculating the rigidity of slender concrete columns:

$$EI = \frac{0.2E_cI_g + E_sI_{se}}{1 + \beta_d} \quad (3)$$

or

$$EI = \frac{0.4E_cI_g}{1 + \beta_d} \quad (4)$$

where

E_c = concrete modulus of elasticity
I_g = gross moment of inertia of the column cross section
E_s = reinforcing bar modulus of elasticity
I_{se} = moment of inertia of the reinforcing bars in the section
β_d = coefficient to account for long-term loading

The ACI Code Commentary states that Eq. (4) was derived for small eccentricity ratios and high levels of axial load where the slenderness effects are most pronounced.

PCI Treatment of Slenderness Effects

The PCI Committee on Prestressed Concrete Columns[13] concluded that Eqs. (3) and (4) cannot be applied directly to prestressed concrete columns and bearing walls. As an alternative, the PCI Committee recommended equations for *EI*, which are based primarily on the work of Nathan (1972-1985). The latest form of these equations (considering short-term loading) is given as:[17]

$$EI = \frac{E_cI_g / \lambda}{1 + \beta_d} \quad (5)$$

$$\lambda = \theta\eta \geq 3.2 \quad (6)$$

$$\eta = 2.5 + 1.6\frac{P}{P_0} \quad (7)$$

where

P = applied axial load on the column from first order analysis
P_0 = pure axial load capacity of the section

Upper and lower limits were specified for η so that it should not be taken less than 6 nor more than 70.

For sections without a compression flange, θ is given by:

$$\theta = \frac{27}{\kappa L / r} - 0.05 \quad (8)$$

where

κ = coefficient for the effective length of the column considering end restraints
L = column length
r = radius of gyration of the cross section

For sections with a compression flange, θ is given by:

$$\theta = \frac{35}{\kappa L / r} - 0.09 \quad (9)$$

Summary of Comparison Between ACI and PCI Methods

It can be observed from the above that the main difference between the ACI and PCI methods is the expression of *EI*; while λ in the ACI method is between 2.5 and 5, it ranges in the PCI method from 3.2 to a value much larger than 5 depending on the slenderness ratio and whether the section is flanged or not.

THEORETICAL FLEXURAL RIGIDITY (*EI*)

Since in practice M_{mid} is not always easy to determine, Eq. (1) is modified to relate M_{end} to the nominal moment, M_n, from sectional analysis, assuming the same axial load. Accordingly, the design nominal moment may be written for the case of equal end moments as:

$$M_n = M_{end}\frac{1}{1 - \frac{P}{P_{cr}}} \quad (10)$$

in which the capacity reduction factors usually added in the ACI Code are not included for the purpose of this discussion. In practice, the code formula should be used.

Eq. (10) may be rearranged to give the critical load for a slender PC column of length L, assuming the remaining variables (P, M_{end}, and M_n) are known:

$$P_{cr} = \frac{P}{1 - \frac{M_{end}}{M_n}} \qquad (11)$$

Recalling that P_{cr} is given by Eq. (2), and equating the two equations yield the following formula for the theoretical effective flexural rigidity, *EI*:

$$EI = \frac{P}{1 - \frac{M_{end}}{M_n}} \frac{L^2}{\pi^2} \qquad (12)$$

In principle, Eq. (12) gives the most accurate value of flexural rigidity, *EI*, that would make M_n predictable from M_{end} or vice-versa. A set of *EI* values may be generated using Eq. (12) in which the M_{end} and P are obtained from finite element analysis, while M_n is obtained from sectional analysis. This approach of extracting the effective *EI* for slender PC and RC columns was commonly followed by several investigators[18,8,15,19] to allow further examination of the effective rigidity.

The main aim of previous studies on flexural rigidity of slender concrete columns as well as this study is to establish an approximate model for *EI* that simulates as closely as possible the theoretical relationship. In some of these studies, notably MacGregor et al.,[18] Nathan,[8] and Mirza,[19] data were collected on effective rigidity for some influencing variables in order to allow a statistical analysis.

In this paper, an alternative approach is followed for determining *EI* using two fundamental concepts that were found to lead to reasonable agreement with the theoretical results from the finite element analysis.

PROPOSED PROCEDURE

The proposed procedure for computing the flexural rigidity, *EI*, for slender PC columns is based on two concepts. The first idea takes advantage of the fundamental relationship between sectional moment and associated curvature. The second concept is based on the tangent modulus of a slender concrete column at onset of buckling under concentric axial compression assuming a nonlinear stress-strain curve of concrete.

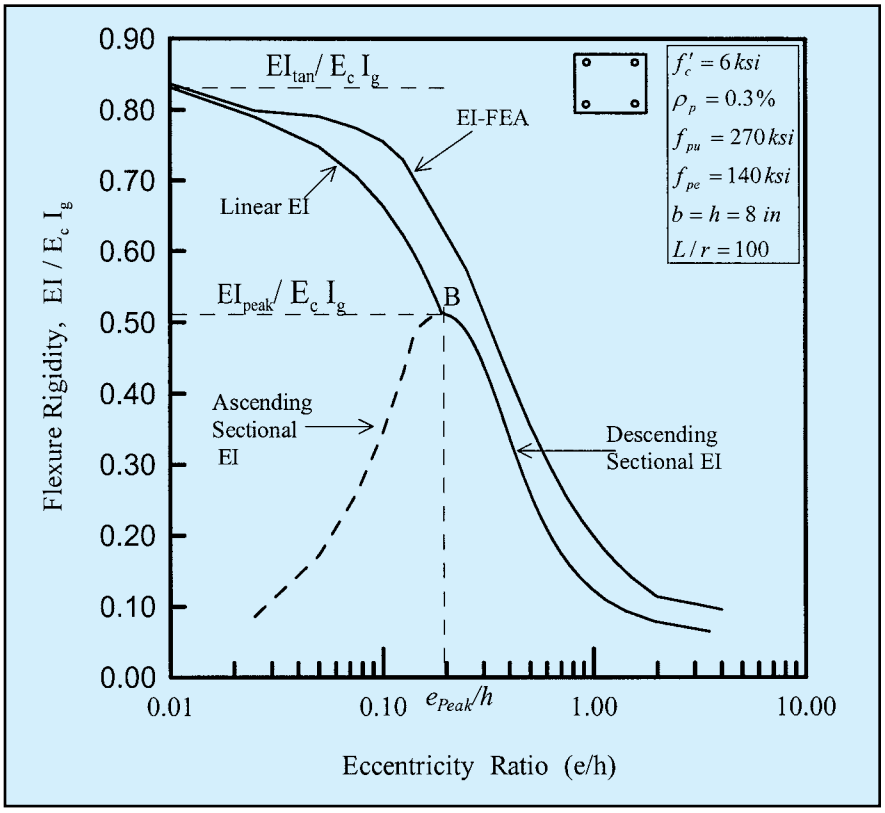

Fig. 3. Proposed *EI* model composed of descending branch of Sectional *EI* and upper portion from linear part. Also shown is *EI* from finite element analysis (FEA) for a slender PC column.

Nominal Bending and Axial Resistance

Regardless of the method used to determine *EI*, the nominal moment and axial load strength envelope of a column section is generally needed for the design of PC columns. It is developed on the basis of equilibrium, strain compatibility, and constitutive relationships. Fig. 2 shows a schematic representation of the calculations for a rectangular cross section having a height, h, and a width, b. The strain distribution is assumed linear over the cross section with a compression limit of 0.003.

For an assumed value of neutral axis depth, c, the strains in any layer of prestressing steel can be computed from:

$$\varepsilon_{pi} = \varepsilon_{pe} + \frac{d_{pi} - c}{c} 0.003 \qquad (13)$$

where

e_{pe} = effective strain in prestressing steel

d_{pi} = depth of a steel layer, i, taken from the compression face

The steel stress, f_{pi}, is found from an appropriate constitutive relationship such as that given in Reference 20, and the stress in concrete is defined as $0.85f'_c$ over an area of $\beta_1 cb$, where β_1 is a factor defined as the ratio of the equivalent rectangular stress block depth to the distance from the extreme compression fiber to the neutral axis depth. Multiplying the stresses in steel and concrete by their corresponding areas, gives the forces in steel and concrete as F_{pi} and C_c, respectively.

Equilibrium requires that the nominal axial load, P_n, and the nominal flexural moment, M_n, be computed respectively from:

$$P_n = C_c - \sum_{1}^{npl} F_{pi} \qquad (14)$$

$$M_n = C_c(h/2 - \beta_1 c/2) + \sum_{1}^{npl} F_{pi}(h/2 - d_{pi}) \qquad (15)$$

where *npl* is the number of prestress-

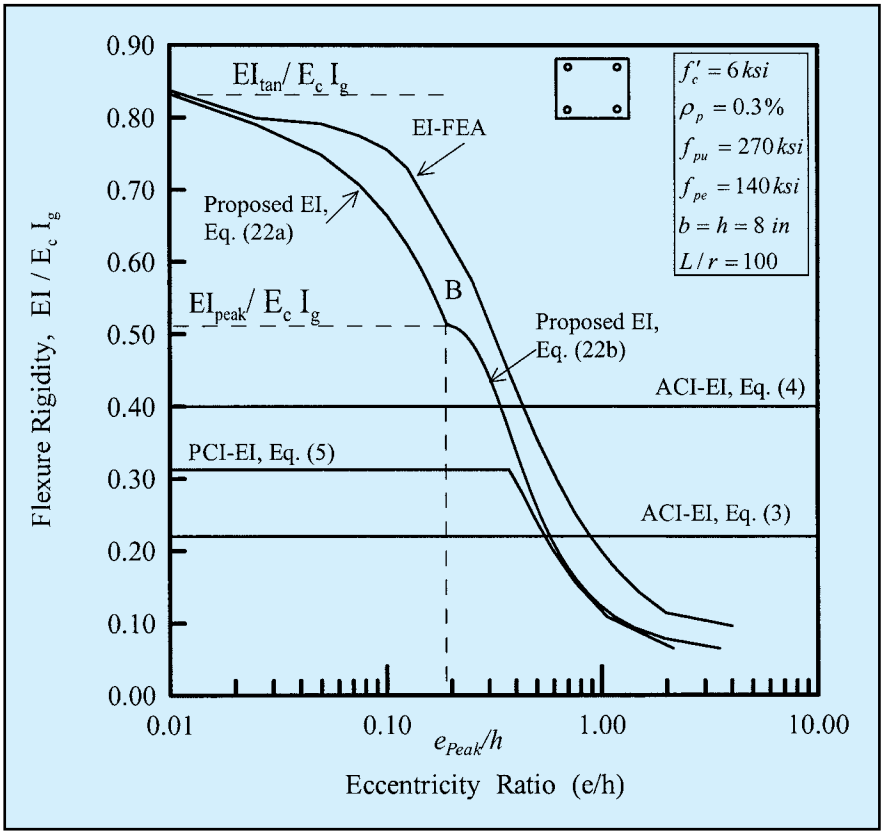

Fig. 4. Comparisons of proposed *EI* model with existing code models and finite element model for a slender PC column (from examples of Appendix B).

ing layers in a section.

Sectional Flexural Rigidity at Nominal Strength

The curvature, ψ_n, at any section at nominal strength can be written as:

$$\psi_n = \frac{M_n}{EI} \qquad (16)$$

The curvature is also defined from compatibility requirements as the ratio of nominal strain at the top of the section to the depth of the neutral axis as shown in Fig. 2. Assuming the compressive strain is equal to 0.003 as per ACI 318, the curvature becomes:

$$\psi_n = \frac{0.003}{c} \qquad (17)$$

By rearranging Eqs. (16) and (17), the flexural rigidity *EI* is computed as:

$$EI = \frac{M_n\, c}{0.003} \qquad (18)$$

The load eccentricity at nominal resistance is defined as:

$$e = \frac{M_n}{P_n} \qquad (19)$$

For different values of c, the nominal bending strength and the flexural rigidity can be computed, respectively, from Eqs. (15) and (18). Then, the flexural rigidity can be plotted versus the eccentricity [from Eq. (19)] leading to an *EI-e* diagram. A typical example is shown in Fig. 3 (derived from the examples of Appendix B), where the rigidity is termed Sectional *EI*, and is compared with the *EI* obtained from finite element analysis [Eq. (12)] and termed EI-FEA.

The Sectional *EI* has an ascending branch that increases to a maximum value (Point B) followed by a descending branch covering a wide range of eccentricities. It can be observed that, while the ascending branch is in total disagreement with the corresponding portion of the EI-FEA curve, the descending branch is very similar to it.

This observation was typical of all the prestressed columns studied. Accordingly, it is believed that the descending branch of the curve may be utilized to model the flexural rigidity *EI* for this range of eccentricities, but a different approach should be used for the smaller eccentricity range.

Note that the concept of using the Sectional *EI* was first introduced in 1990 (Reference 15) for PC columns and was also discussed in 1992 by Zeng et al.[21] for reinforced concrete columns. However, Zeng et al.[21] did not distinguish between the ascending and descending branches of the *EI-e* curve.

Sectional Rigidity and Eccentricity at Peak Point

The boundary of the descending branch may be determined either by inspection when sufficient numerical values are generated, or by using an expression that gives the neutral axis associated with the value of *EI* at the peak point (Point B in Fig. 3). Analytically, this can be achieved by differentiating *EI* with respect to c and equating the derivative to zero.

This leads to the neutral axis depth at which flexural rigidity reaches its maximum value; for a rectangular section it is:

$$c_{peak} = \frac{2h}{3\beta_1} \qquad (20)$$

in which h is the total depth of the section.

Analyzing the section with $c = c_{peak}$ and computing M_n and P_n from Eqs. (14) and (15) allow for calculating EI_{peak} using Eq. (18) and the corresponding e_{peak} using Eq. (19).

Linear *EI* Method for Small Eccentricity Range ($e < e_{peak}$)

The ascending part of the Sectional *EI* presented in Fig. 3 (up to Point B) is in total disagreement with the theoretical *EI* from the finite element analysis. The apparent reason for this

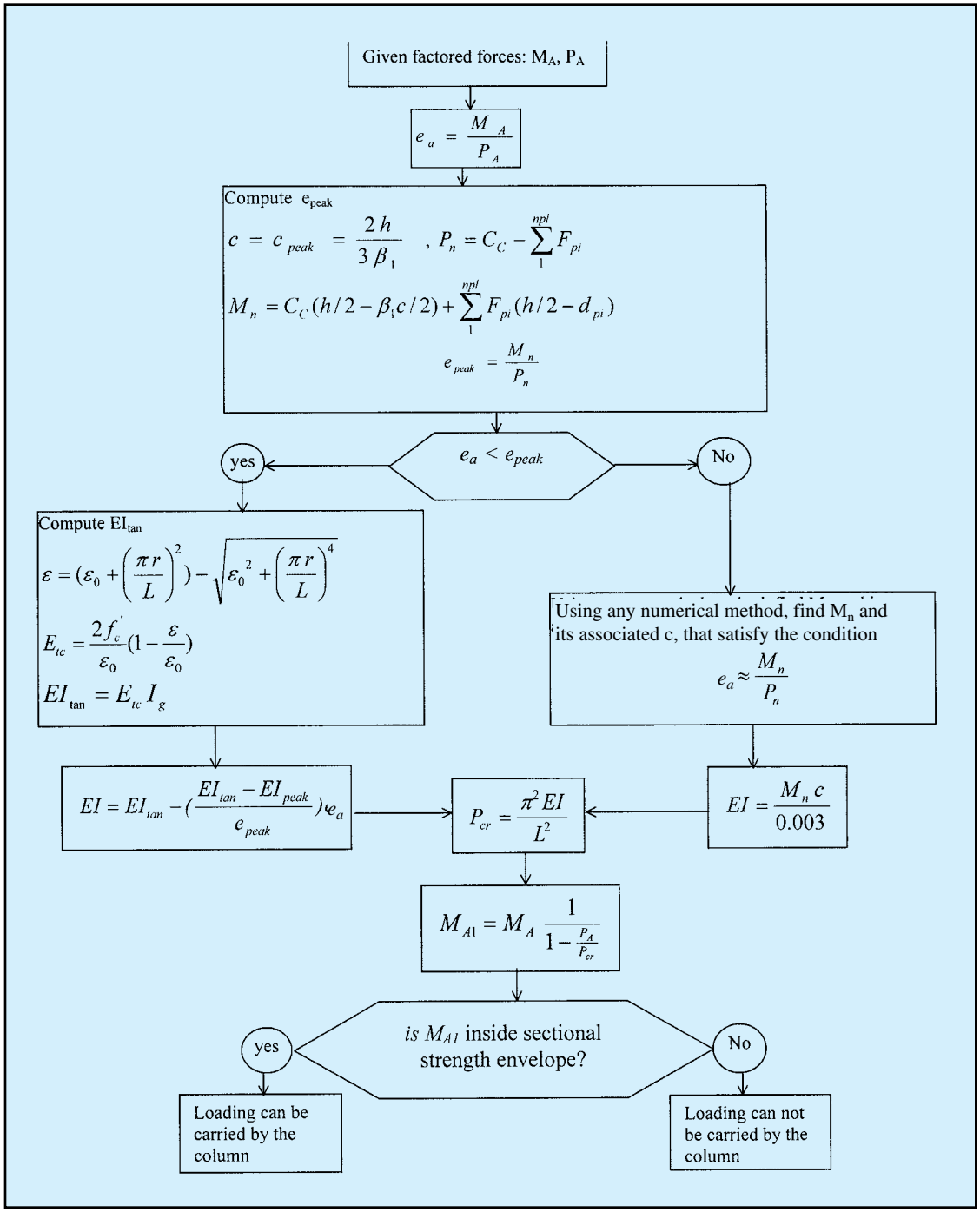

Fig. 5. Flowchart for implementing the proposed model for a slender column under equal end moments ignoring all reduction factors.

is that under small eccentricities column failure is initiated by stability at relatively lower strains, while the section analysis assumes material failure at a relatively larger strain.

Therefore, the ascending branch is not applicable for eccentricities smaller than the peak eccentricity. However, it is believed that the use of the tangent modulus of a slender PC column under pure compressive axial load can help in developing an approximate *EI* expression for this range of eccentricities; first, let us define:

$$(EI)_{tan} = E_{tc} I_g \qquad (21)$$

where E_{tc} is the tangent modulus of concrete, given later by Eq. (27), and I_g is the gross moment of inertia of the column cross section.

The derivation of this equation is given in Appendix A. In the following discussion, only the end result is provided.

In summary, the proposed flexural rigidity is given by:

$$EI = \begin{cases} EI_{tan} - \left(\frac{EI_{tan} - EI_{peak}}{e_{peak}}\right)e & e \le e_{peak} \quad (22a) \\ \frac{M_n c}{0.003} & e > e_{peak} \quad (22b) \end{cases}$$

Eq. (22) represents the *EI* model proposed in this study for PC col-

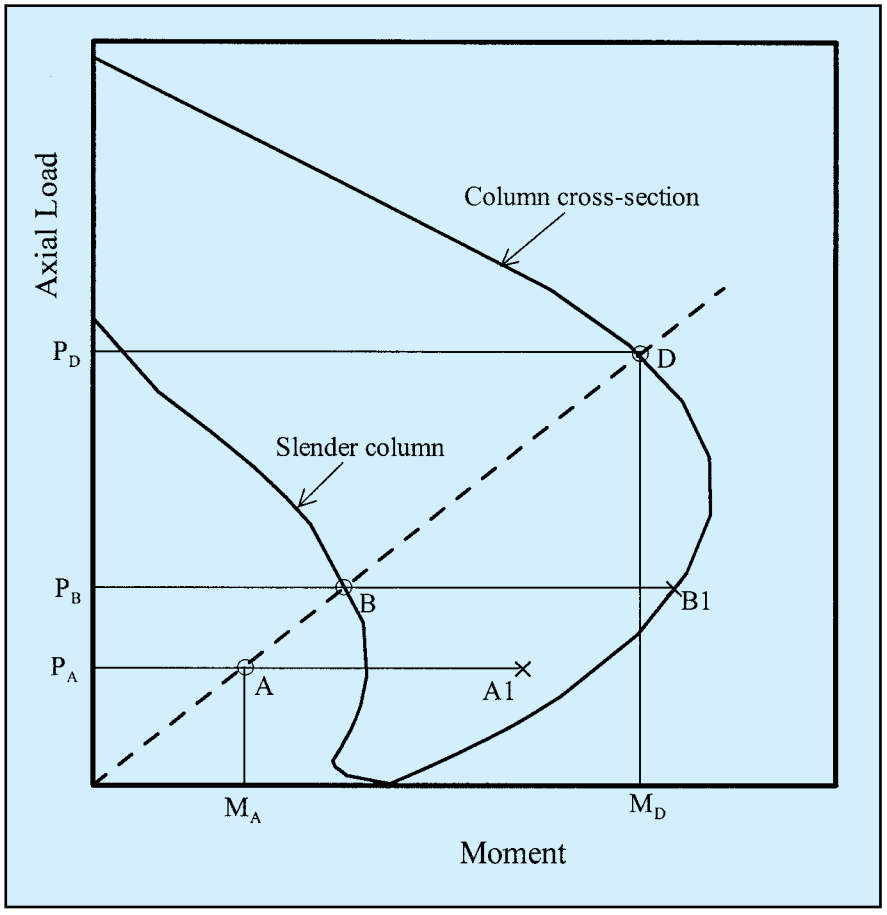

Fig. 6. Implementing proposed model for two cases: (1) Checking the adequacy for a given loading at Point A; (2) Locating Point B based on knowing Point D.

umns; it is plotted in Fig. 4 for a typical slender PC column. The curve comprises two parts with minor discontinuity at e_{peak}. The *EI* from the finite element analysis is also plotted on the same figure for comparison (EI-FEA). A very good agreement in both trend and numerical values is observed between the two curves even though they were developed independently.

The current ACI 318 equations are also plotted in Fig. 4 and identified as ACI-EI Eqs. (3) and (4), respectively. They show a complete insensitivity to a wide change in eccentricity, and are too conservative at small eccentricities and unsafe at larger eccentricities.

Finally, the PCI recommendations represented by Eq. (5) are shown in the figure for comparison. For $e/h < 0.13$, Eq. (5) is extremely conservative, however, beyond that, it is in close agreement with the proposed *EI* in both trend and numerical values.

IMPLEMENTATION OF PROPOSED PROCEDURE

In the proposed method, the eccentricity of loading plays a major role in determining *EI* as illustrated next for different situations. Fig. 5 shows two paths for the calculations depending on e_{peak}. When the applied eccentricity is less than the peak eccentricity, the linear *EI* in Eq. (22a) must be used. On the other hand, when the applied eccentricity is larger than the peak eccentricity, the Sectional *EI* in Eq. (22b) must be used.

Once the *EI* is known, the method is similar to the ACI Code method (or PCI recommendations) and the same procedure may be followed. It should be noted that in the flowchart and the examples solved in this paper, all the reduction factors and the long-term factor were dropped for clarity sake, but they can be restored for actual designs.

Checking the Adequacy of Column Strength Under a Given Loading

Assume that a long column is subjected to a factored equal end moment, M_A, and an axial load, P_A; determine whether the column is capable of carrying such a load. The loading is shown in Fig. 6 as Point A.

The eccentricity of the applied loading $e_a = M_A/P_A$ is first compared with e_{peak}. Example 2 in Appendix B illustrates the computation of e_{peak}.

Assume it is found that $e_a \le e_{peak}$. Then, one needs to compute EI_{tan} and EI_{peak} and use Eq. (22a). Example 1 in Appendix B shows how to compute EI_{tan}, while Example 2 shows how to compute EI_{peak}.

Once *EI* is obtained, the critical load at the eccentricity e_a is computed from Eq. (2), and the magnified moment is calculated from Eq. (10). The magnified moment is compared with the sectional moment at the same axial load, P_A. Note that Example 3 of Appendix B provides a numerical example illustrating this situation.

Assume it is found that $e_a \ge e_{peak}$. For this situation, *EI* is computed based on the nominal moment at Point D, M_D, and the associated c in accordance with Eq. (22b). Locating Point D may require some interpolation when a sufficient number of (M_n, P_n) points are generated for the section.

Alternatively, an iterative procedure may be followed by assuming c and computing M_n, and P_n until $e_a \approx M_n/P_n$. Hence, *EI* is computed by Eq. (22b) after substituting the values of c and M_n. The remaining steps are as indicated above, and as illustrated in Example 4 of Appendix B.

Developing Points on the Interaction Diagram for a Slender PC Column

For illustration purposes, Point B, shown in Fig. 6 on the slender PC column interaction diagram, is to be evaluated based on Point D of the sectional interaction diagram. At Point D, the eccentricity is $e = M_D/P_D$. When e is greater than e_{peak}, *EI* is computed using Eq. (22b) by substituting c and M_D at that point.

On the other hand, if e is smaller than or equal to e_{peak}, *EI* is computed using the linear form Eq. (22a). Based on *EI*, the critical load is evaluated for

that eccentricity using Eq. (2).

Knowing P_{cr} and the associated e, the desired point on the slender load-moment interaction diagram (M_B,P_B) may be obtained by successive approximation. The main equation for finding this solution is obtained by rearranging Eq. (10) such that:

$$P_B = \frac{P_{cr}}{1 + \frac{P_{cr}\, e}{M_{B1}}} \qquad (23)$$

Satisfying Eq. (23) begins by assuming that $M_{B1} = M_D$ and solving for an approximate value for P_B. In general, the resulting value of P_B is a reasonable estimate leading to the correct value. However, to improve the prediction, additional iterations can be carried out. Given P_B, the associated moment M_{B1} from sectional analysis is obtained, then substituted in Eq. (23) leading to an improved estimate of P_B.

This process may be repeated for a few cycles until the change in P_B is within an acceptable limit, which indicates convergence. After convergence is obtained, the moment associated with P_B is $M_B = P_B e$ which represents Point B in Fig. 6. Example 5 of Appendix B illustrates this process for a typical point. The above approach was used to generate data for the parametric analyses presented in the following section.

APPLICATION AND COMPARISON

The proposed *EI* model was used to generate end moment versus axial load interaction diagrams for a number of slender columns having prestressed reinforcement ratios between 0.2 to 0.5 percent. A typical square [8 x 8 in. (103 x 103 mm)] simply supported slender PC column is considered with equal end eccentricity as illustrated in Fig. 1. For these applications, all reduction factors are ignored and short-term loading is considered. A computer program was written to carry out the computations for a practical range of values of the main parameters.

Connecting twenty independent pairs of end moment and axial load points generated the end moment versus axial load envelope from the fi-

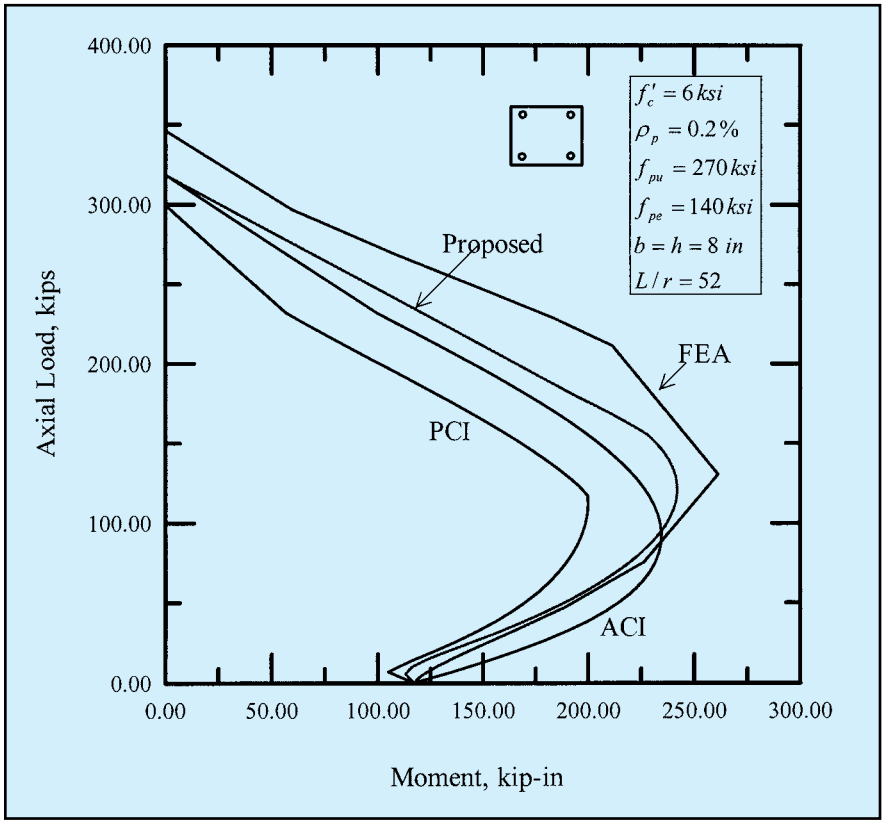

Fig. 7. Comparison of interaction diagrams developed on basis of flexural rigidities suggested by the current study, ACI 318, and PCI with finite element analysis (FEA) for $L/r = 52$ and $\rho_p = 0.2$ percent.

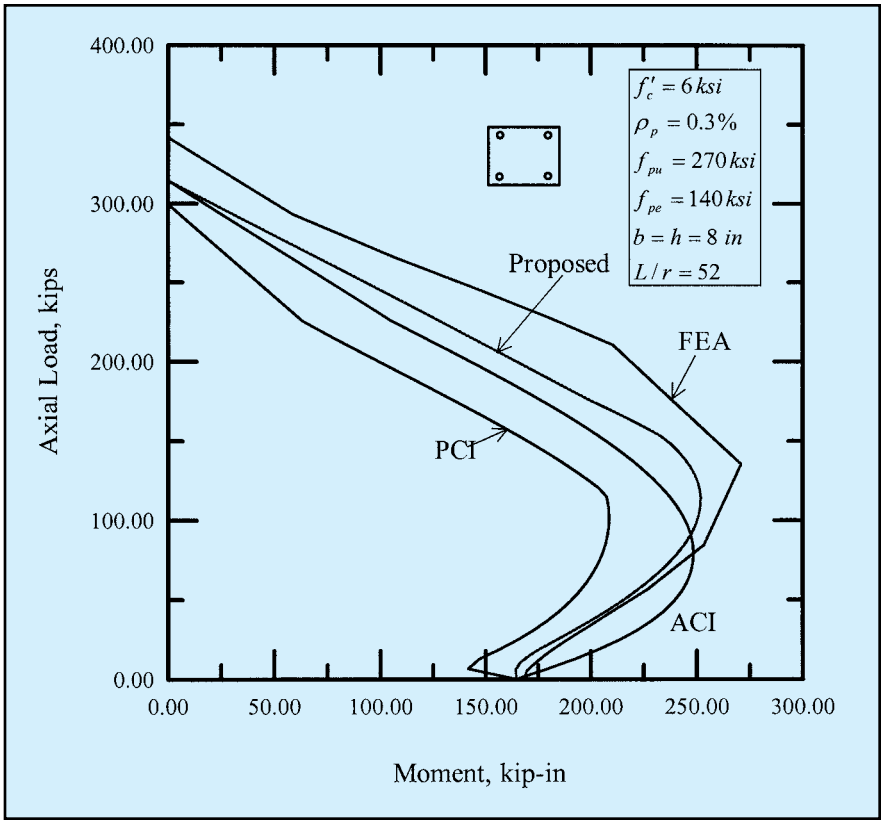

Fig. 8. Comparison of interaction diagrams developed on the basis of flexural rigidities suggested by current study, ACI 318, and PCI with finite element analysis (FEA) for L/r =52 and $\rho_p = 0.3$ percent.

Table 1. Summary of results for slenderness ratio (L/r) = 52.

Method of computing *EI*	Maximum load	Balanced point	
		ρ_p = 0.2 percent	ρ_p = 0.3 percent
Proposed	$1.0P_0$	$(2.1M_0, 0.37P_0)$	$(1.53M_0, 0.36P_0)$
ACI	$1.0P_0$	$(2.0M_0, 0.29P_0)$	$(1.51M_0, 0.25P_0)$
PCI	$0.95P_0$	$(1.71M_0, 0.34P_0)$	$(1.27M_0, 0.33P_0)$

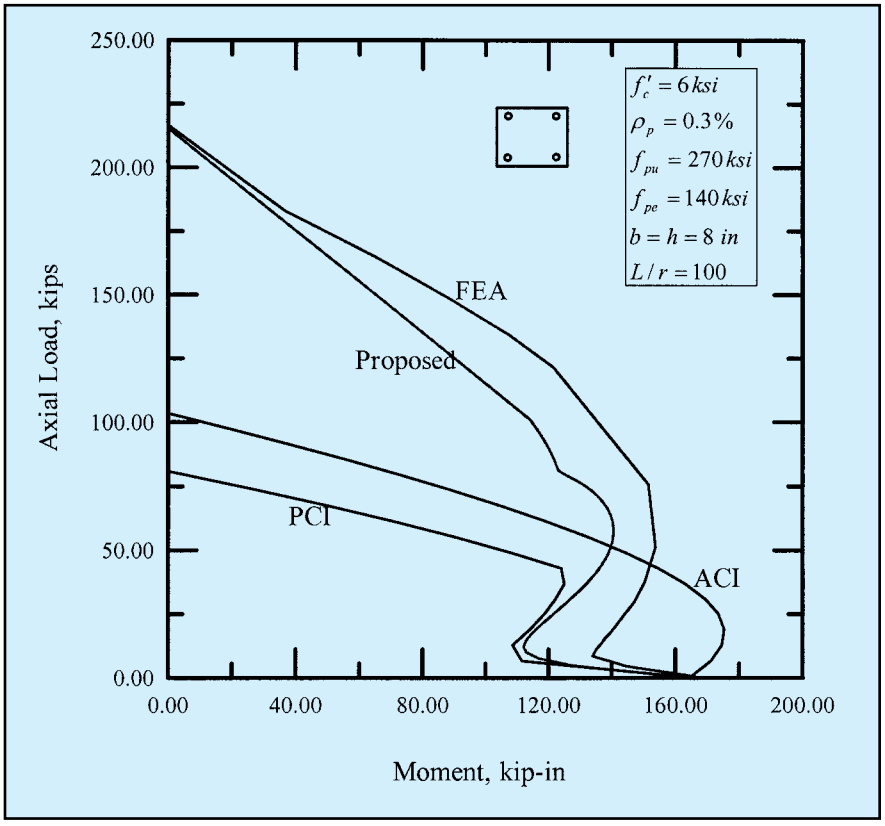

Fig. 9. Comparison of interaction diagrams developed on basis of flexural rigidities suggested by current investigation, ACI 318, and PCI with finite element analysis (FEA) for L/r = 100 and ρ_p = 0.3 percent.

nite element analysis. A typical point is obtained by applying moment and axial load to the column ends in incremental form using a computer program developed earlier.[15] The program is based on the well-known finite element principles with consideration to material and geometric nonlinearities. The method carries no assumption related to or utilization of the magnification formula.

Along with the proposed approximate method and the finite element analysis, the current *EI* models recommended by the ACI Building Code, Eq. (4), and PCI recommendations, Eq. (5), were both used to generate end moment versus axial load interaction diagrams.

Comparisons were made with the results obtained from the proposed model (Proposed), finite element analysis (FEA), current code recommendations (ACI and PCI), and experimental test results. Having the four methods represented concurrently for each case help broaden our understanding of their capabilities and limitations.

Columns with Slenderness Ratio (L/r) = 52

The moment versus axial load interaction diagram based on the proposed *EI* method is presented in Fig. 7 for a column with a prestressed reinforcement ratio of 0.2 percent; it has two branches with a distinctive balance point having coordinates of $0.37P_0$ and $2.1M_0$, where P_0 is the nominal concentric axial load capacity of the section, and M_0 is the nominal flexural moment capacity of the section at zero axial load.

The upper branch reaches a maximum value of P_0 and the entire branch is on the conservative side of the curve predicted by FEA. For the lower branch, the decrease in axial load is associated with a decrease in moment and the branch is very close in shape and value to the FEA curve. Fig. 8 shows the curves for the same column with a 0.3 percent prestressed reinforcement ratio and a similar trend is observed.

The curve generated using the ACI method for ρ_p = 0.2 percent has two branches similar to the proposed method with a balance point having an axial load of $0.29P_0$ and a moment of $2.0M_0$. While the upper branch is in agreement with the proposed method and on the conservative side, the lower branch predicts higher strengths and it is on the unsafe side with respect to the FEA results. Increasing the percentage of prestressing steel affects the balanced moment as shown in Fig. 8 and Table 1 but leads to similar trends.

The curve generated from the PCI approach for ρ_p = 0.2 percent has slightly different features (see Fig. 7). The balanced point has coordinates of $0.34P_0$ and $1.71M_0$. This curve has a noticeable middle branch where the drop in axial load from $0.4P_0$ to $0.21P_0$ occurs without much of a change in moments. Below $0.21P_0$, the moment decreases until it reaches a minimum value of $0.86M_0$ at $0.02P_0$ before increasing again to M_0. This curve represents the most conservative method among the four approaches shown in the figure. Similar observations can be made for ρ_p = 0.3 percent as shown in Fig. 8 and Table 1.

Columns with Slenderness Ratio (L/r) = 100

This is a square column such as described in the examples of Appendix A. The moment versus load interaction curve generated by the proposed method for ρ_p = 0.3 percent is shown in Fig. 9; it shows three parts: the upper part starts at a maximum load of $0.68P_0$ and extends linearly to the point defined by e_{peak} at which the axial load is $0.26P_0$ and the moment is

$0.75M_0$.

Below this part comes the middle part, which extends in a nonlinear form to a point with coordinates $0.04P_0$ and $0.68M_0$. The lower part extends to the pure flexure case in a linear form. As ρ_p is increased to 0.4 and 0.5 percent (see Figs. 10 and 11), respectively, the main change occurs in the middle part, which becomes flatter.

Overall, these strength envelopes have similar shapes to the corresponding curves from FEA and are on the conservative side except for the concentric load, which is nearly identical to that computed by FEA. Table 2 shows the numerical coordinates of the key points for these cases.

The curve generated by the ACI method for ρ_p = 0.3 percent has a maximum load of $0.14P_0$. Compared to the FEA curve, it underestimates strength for loads higher than $0.14P_0$ and overestimates the strength for loads lower than $0.14P_0$. Moreover, the overall shape of the curve is in disagreement with the trend established by FEA and confirmed by the proposed model. Similar observations are made when ρ_p is increased to 0.4 and 0.5 percent as shown in Figs. 10 and 11, respectively.

The curve generated by the PCI method for ρ_p = 0.3 percent is characterized by three distinctive parts. The maximum axial load is $0.26P_0$, which constitutes only 37 percent of that predicted by FEA. The middle part is characterized by a steep drop in axial load with a slight variation in moments; it starts from axial load of $0.14P_0$ and the moment of $0.77M_0$, and extends to a point of $0.04P_0$ and $0.66M_0$ before the moment increases to M_0 at zero axial load. The middle part of the diagram becomes more conservative as ρ_p is increased to 0.4 and 0.5 percent, as shown in Figs. 10 and 11, respectively.

COMPARISON WITH TEST RESULTS

The finite element analysis model used to verify the proposed *EI* model of this study was compared with the results of 121 column tests obtained from various sources in the technical literature.[6,21,11] A summary of the test

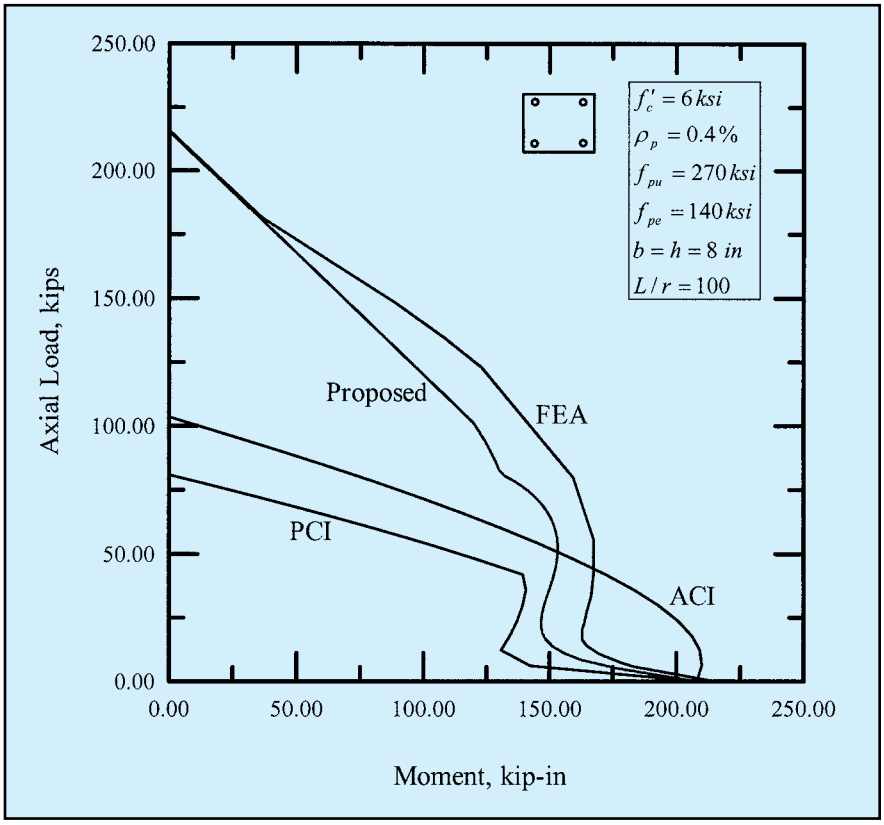

Fig. 10. Comparison of interaction diagrams developed on basis of flexural rigidities suggested by current investigation, ACI 318, and PCI with finite element analysis (FEA) for L/r =100 and ρ_p = 0.4 percent.

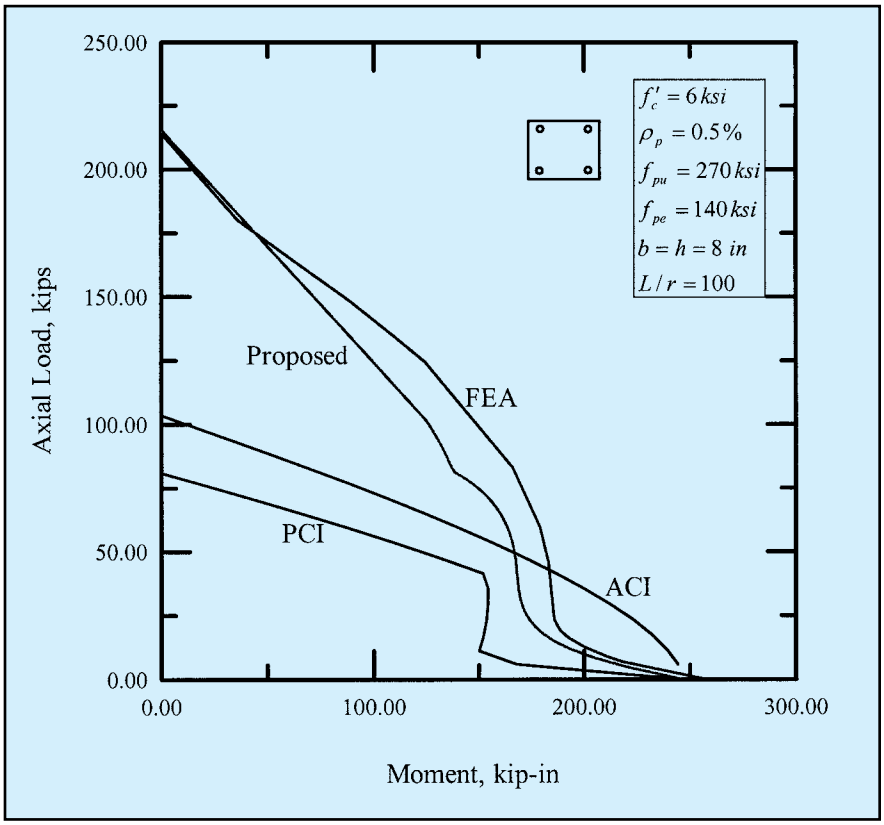

Fig. 11. Comparison of interaction diagrams developed on basis of flexural rigidities suggested by current study, ACI 318, and PCI with finite element analysis (FEA) for L/r = 100 and ρ_p = 0.5 percent.

Table 2. Critical points on interaction diagrams for slender PC columns (L/r) = 100.

Method of computing *EI*	ρ_p = 0.4 percent			ρ_p = 0.5 percent		
	Max. *P*	Middle point	Lower point	Max. *P*	Middle point	Lower point
Proposed	$0.69P_0$	$(0.62M_0, 0.27P_0)$	$(0.71M_0, 0.06P_0)$	$0.7P_0$	$(0.56M_0, 0.26P_0)$	$(0.71M_0, 0.075P_0)$
ACI	$0.33P_0$	$(0.80M_0, 0.14P_0)$	—	$0.34P_0$	$(0.76M_0, 0.14P_0)$	—
PCI	$0.26P_0$	$(0.67M_0, 0.14P_0)$	$(0.63M_0, 0.04P_0)$	$0.26P_0$	$(0.61M_0, 0.13P_0)$	$(0.61M_0, 0.04P_0)$

Table 3. Summary of comparison with test results of PC columns.

Source of tests	No. of tests	Average of P_{test}/P_{FEA}	No. of columns for which the P_{FEA} is within			
			5 percent	10 percent	15 percent	20 percent
Aroni[6]	36	1.052	13	23	32	33
Carinci and Halvorsen[21]	36	0.955	20	29	35	36
Yuan's concentric-short columns[11]	27	0.960	12	23	27	27
Yuan's long columns[11]	22	1.047	6	16	19	22
Total	121	1.00	51	91	113	118

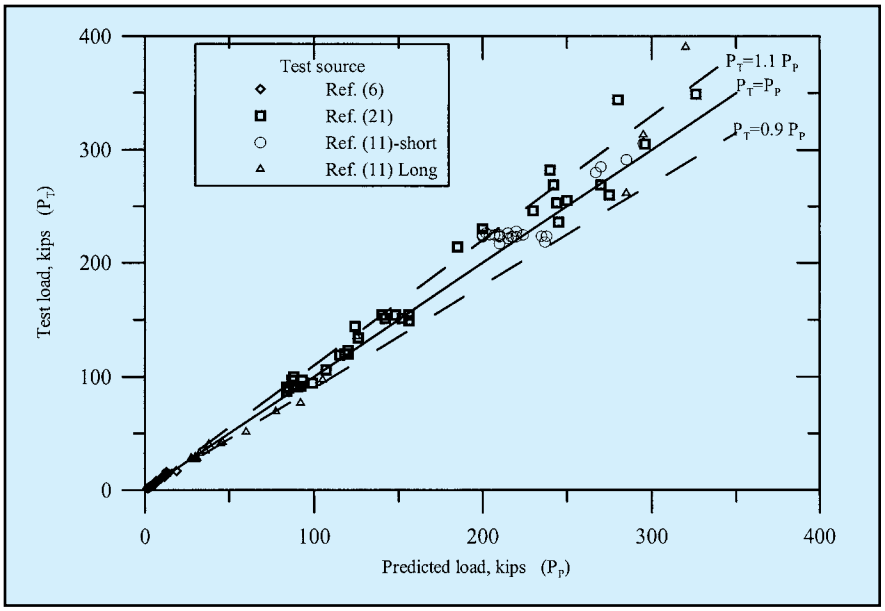

Fig. 12. Finite element predicted load versus test load at failure for 121 slender columns obtained from technical literature.

results is shown in Table 3.

The average of the P_{test} to P_{FEA} ratio is shown for each group of tests having a range of 0.955 to 1.052 with an overall average ratio of 1.0. The breakdown of prediction accuracy is illustrated in the table. The predicted load versus the test load for all of the columns is presented in Fig. 12.

Table 3 and Fig. 12 confirm first the validity of the finite element model (FEA) used to conduct the predictions. Reasonable differences between predicted and experimental results are understandable due to a number of influencing factors, which include uncertainty in material properties and the constitutive relationships. Also during the testing, accidental eccentricity or restraints due to friction at the ends of columns may have significant effects on the ultimate load. It was observed, for instance, that two otherwise identical columns led to ultimate loads that are different by 12 percent.

Six slender prestressed concrete columns tested by Carinci and Halvorsen in 1986[22] were chosen to illustrate the predictive capability of the different methods considered in this study. They are selected to represent an important case of low reinforcement ratio and high slenderness.

Three of the columns are among those predicted with a 5 percent accuracy and the other three are from those predicted with a 10 percent accuracy. The results for six columns are shown in Fig. 13 along with the FEA generated curve, the proposed curve, the ACI 318 Eq. (4) curve, and the curve based on the PCI recommendations.

The tests confirm the overall accuracy of the upper branch of the proposed method, despite some overestimated predictions that are considered within a reasonable limit as discussed earlier. The test results also confirm the degree of conservatism in the predictions based on ACI 318 or the PCI recommendations. Note that for comparison purposes, no reduction factors were used in any curve prediction.

CONCLUDING REMARKS

A comprehensive nonlinear finite element analysis suggests that the flexural rigidity, *EI*, of prestressed concrete columns varies widely with the load eccentricity and other material and reinforcement parameters such as concrete strength, prestress level, reinforcement ratio and slenderness ratio. This variability is so complex that it cannot be described adequately by a simple formula such as that attempted in the ACI Code or the PCI recommendations.

The methodology proposed in this paper to estimate the flexural rigidity requires moderate analytical effort; it simulates very well the predicted analytical results while also incorporating results from experimental tests. Once the flexural rigidity is determined, the proposed method offers the advantage to simply integrate in the generally accepted procedure of the ACI Code to determine the critical buckling load used in the magnification formula, and thus to allow a prediction of nominal resistance.

In comparison to predictions from

the finite element analysis, the proposed method incorporates both trends and values significantly better than either the ACI Code formula or the PCI recommendations. The effective rigidity using the ACI Code shows very little resemblance to the rigidity obtained from theoretical considerations.

The effective rigidity using the PCI recommendations is generally on the safe side; however, it is too conservative particularly in the low eccentricity range and higher slenderness ratios. While the PCI approach is certainly acceptable for design, the corresponding safety margin may be too large in some cases.

Since the proposed method described here provides a better answer overall without sacrificing safety, it is recommended for inclusion in future versions of the ACI Code; it is also recommended as a tentative procedure to replace the PCI recommendations to determine the flexural capacity of prestressed concrete columns throughout the range of slenderness ratios.

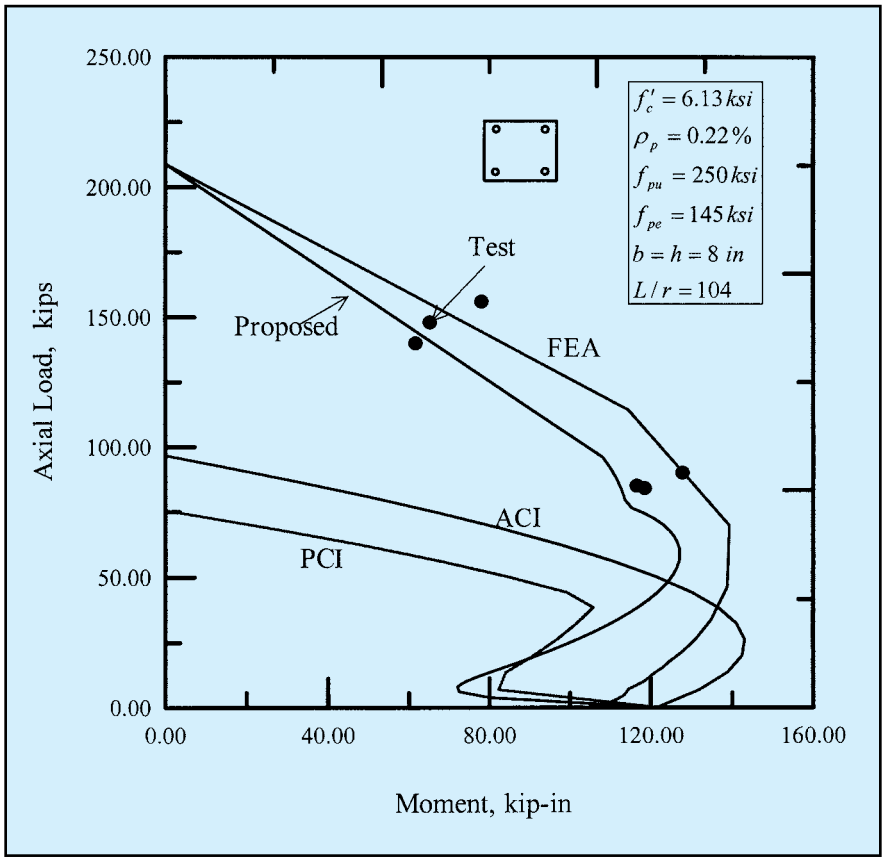

Fig. 13. Comparison of interaction diagrams developed on basis of flexural rigidities suggested by current study, ACI 318, and PCI with finite element analysis (FEA) and test results for L/r = 104 and ρ_p = 0.22 percent.

ACKNOWLEDGMENT

REFERENCES

The research work of the first author was supported by a fellowship award from King Saud University, Saudi Arabia. The research work of the second author has been supported in the past by numerous grants from the National Science Foundation and by the University of Michigan. Their support is gratefully acknowledged.

The authors would also like to thank the PCI JOURNAL reviewers of the first draft of this paper for their constructive comments.

1. Lin, T. Y., and Itaya, R., "A Prestressed Concrete Column Under Eccentric Loading," PCI JOURNAL, V. 2, No. 3, May-June 1957, pp. 5-17.
2. Zia, P., and Moreadith, F. L., "Ultimate Load Capacity of Prestressed Concrete Columns," *ACI Journal*, V. 63, July 1966, pp. 767-786.
3. Brown, H. R., and Hall, A. S., "Tests on Slender Prestressed Concrete Columns," Symposium on Reinforced Concrete Columns, SP-13, American Concrete Institute, Farmington Hills, MI, 1966, pp. 179-192.
4. Kabaila, A. P., and Hall , A. S., "Analysis of Instability of Unrestrained Prestressed Concrete Columns with End Eccentricities," Symposium on Reinforced Concrete Columns, SP-13, American Concrete Institute, Farmington Hills, MI, 1966, pp. 157-178.
5. Aroni, S., "Slender Prestressed Concrete Columns," Report No. 67-10, Structural Engineering and Structural Mechanics, College of Engineering, University of California, Berkeley, CA, 1967, 237 pp.
6. Aroni, S., "Slender Prestressed Concrete Columns," *Journal of the Structural Division*, ASCE, V. 94, ST4, April 1968, pp. 875-904.
7. Nathan, N. D., "Slenderness of Prestressed Concrete Beam-Columns," PCI JOURNAL, V. 17, No. 6, November-December 1972, pp. 45-57.
8. Nathan, N. D., "Applicability of ACI Slenderness Computations to Prestressed Concrete Sections," PCI JOURNAL, V. 20, No. 3, May-June 1975, pp. 68-85.
9. Nathan, N. D., "Slenderness of Prestressed Concrete Columns," PCI JOURNAL, V. 28, No. 2, March-April 1983, pp. 50-77.
10. Nathan, N. D., "Rational Analysis and Design of Prestressed Concrete Columns and Wall Panels," PCI JOURNAL, V. 30, No. 3, May-June 1985, pp. 82-133.
11. Yuan, R. L., "Prestressed Concrete Column Behavior," Final Report, PCI Research Project No. 3, Prepared for Prestressed Concrete Institute by Department of Civil Engineering, The University of Texas at Arlington, Arlington, TX, 1987, 191 pp.
12. Issa, M., and Yuan, R., "Prestressed Concrete Column Behavior," PCI JOURNAL, V. 34, No. 6, November-December 1989, pp. 51-67.
13. PCI Committee on Prestressed Concrete Columns, "Recommended Practice for the Design of Prestressed Concrete Columns and Walls," PCI JOURNAL, V. 33, No. 4, July-August 1988, pp. 56-95.
14. Shuraim, A. B., and Naaman, A. E., "Analysis of Slender Prestressed Concrete Columns," ASCE Seventh Structures and Pacific Rim Engineering Congress, Volume on *Analysis, Design, and Testing*, A. S-H. Ang, Editor, San Francisco, CA, 1989, pp. 231-240.
15. Shuraim, A. B., "Slenderness Effects in Prestressed Concrete Columns," Ph. D. Dissertation, The University of Michigan, Ann Arbor, MI, 1990.
16. ACI Committee 318, "Building Code Requirements for Reinforced Concrete (ACI 318)," American Concrete Institute, Farmington Hills, MI, 1995.
17. *PCI Design Handbook – Precast and Prestressed Concrete*, Fifth Edition, Precast/Prestressed Concrete Institute, Chicago, IL, 1999.
18. MacGregor, J. G., Oelhafen, U. H., and Hage, S. E., "A Re-Examination of the *EI* Value for Slender Columns," Symposium on Reinforced Concrete Columns, SP-50, American Concrete Institute, Farmington Hills, MI, 1975, pp. 1-40.
19. Mirza, S. A., "Flexural Stiffness of Rectangular Reinforced Concrete Columns," *ACI Structural Journal*, V. 87, No. 4, July-August 1990, pp. 425-435.
20. Menegotto, M., and Pinto, P. E., "Method of Analysis for Cyclically Loaded R. C. Plane Frames," IABSE Preliminary Report for Symposium on Resistance and Ultimate Deformability of Structures Acted on Well-Defined Repeated Loads, Lisbon, Portugal, 1973, pp. 15-22.
21. Zeng, J. M., Duan, L., Wang, F. M., and Chen, W. F., "Flexural Rigidity of Reinforced Concrete Columns," *ACI Structural Journal*, V. 89, No. 2, March-April 1992, pp. 150-158.
22. Carinci, C. A., and Halvorsen, G. T., "Tie Requirements for Prestressed Concrete Columns," Final Report, Department of Civil Engineering, West Virginia University, October 1984 (Revised July 1986), 93 pp.
23. Gere, J., and Timoshenko, S. P., *Mechanics of Materials*, Third SI Edition, Chapman & Hall, London, United Kingdom, 1991.
24. Shanley, F. R., "Inelastic Column Theory," *Journal of the Aeronautical Sciences*, V. 14, No. 5, May 1947, pp. 261-267.

APPENDIX A — DERIVATIONS OF EI_{tan}

25. Hognestad, E., "A Study of Combined Bending and Axial Load in Reinforced Concrete Members," University of Illinois Engineering Experiment Station, Bulletin Series No. 399, Bulletin No. 1, Urbana-Champaign, IL, 1951, 28 pp.
26. Ahmed, S. H., "Properties of Confined Concrete Subjected to Static and Dynamic Loading," Ph. D. Thesis, Department of Materials Engineering, University of Illinois at Chicago, Chicago, IL, 1981, 342 pp.

Following the tangent modulus theory,[23,24] the buckling load for a hinged prestressed concrete column considering nonlinear properties of the materials is given by:

$$P_{cr} = \frac{\pi^2 (E_{tc} I_c + E_{tp} I_p)}{L^2} \tag{24}$$

where

E_{tc} = tangent modulus of concrete
E_{tp} = tangent modulus of steel reinforcement
I_c = moment of inertia of concrete
I_p = moment of inertia of steel reinforcement cross section

Equilibrium and compatibility conditions lead to:

$$P_{cr} = A_c E_{sc} \varepsilon - A_p E_{sp} (\varepsilon_{pe} - \varepsilon) \tag{25}$$

where

E_{sc} = secant modulus of concrete
E_{sp} = secant modulus of steel reinforcement
A_c = cross-sectional area of concrete
A_p = cross-sectional area of steel reinforcement
ε_{pe} = effective strain in prestressing steel

Since the area of steel is generally small, the contribution of the steel can be neglected from both equations. Consequently, Eqs. (24) and (25) can be combined to produce Eq. (26):

$$P_{cr} = \frac{\pi^2 E_{tc} I_g}{L^2} = A_g E_{sc} \varepsilon \tag{26}$$

where

I_g = moment of inertia of cross section
A_g = area of gross cross section

The concrete tangent modulus E_{tc} can be obtained by differentiating the stress-strain relationship with respect to strain. Using, for instance, the parabolic equation suggested by Hognestad[25] leads to:

$$E_{tc} = \frac{2 f'_c}{\varepsilon_0} \left(1 - \frac{\varepsilon}{\varepsilon_0} \right) \tag{27}$$

where ε_0 is the concrete strain at maximum strength.

For normal weight concrete, ε_0 can be estimated by the following expression:[26]

$$\varepsilon_0 = 0.001648 + 0.000114 f'_c \tag{28}$$

in which f'_c is in ksi units.

Similarly, the concrete secant modulus E_{sc} at a particular strain can be obtained by dividing the stress in the stress-strain relationship by the strain**.** Using the parabolic relationship of Hognestad leads to:

$$E_{sc} = \frac{f'_c}{\varepsilon_0} \left(2 - \frac{\varepsilon}{\varepsilon_0} \right) \tag{29}$$

Substituting the expressions of E_{tc} and E_{sc} into Eq. (26) and solving for the strain leads to:

APPENDIX B — NUMERICAL DESIGN EXAMPLES

$$\varepsilon = \left[\varepsilon_0 + \left(\frac{\pi r}{L}\right)^2\right] - \sqrt{\varepsilon_0^2 + \left(\frac{\pi r}{L}\right)^4} \qquad (30)$$

Solving Eq. (30) and substituting the resulting strain in Eq. (27) leads to what is defined here as the concrete tangent modulus for a given slender column under concentric axial load. The tangent flexural rigidity is obtainable by substituting E_{tc} and the gross moment of inertia for the cross section, I_g, into Eq. (21), that is:

$$(EI)_{tan} = E_{tc} I_g \qquad (21)$$

The five examples presented in this Appendix are in reference to a slender column simply supported with equal end eccentricity as shown in Fig. 1. For these examples, all reduction factors are ignored and short-term loading is considered.

Geometrical data: L = 231 in., section area = 8 x 8 sq in., $r = 0.29h$ = 2.31 in., L/r = 100.

Material data: f'_c = 6 ksi, ρ_p = 0.3 percent, f_{pu} = 270 ksi, f_{pe} = 140 ksi.

For the section under consideration, several points of the axial load versus moment interaction diagram are presented in Table B1. The table also gives the eccentricity and the Sectional *EI* for each point and was used to develop Figs. 3 and 4.

EXAMPLE 1: Shows How Concentric Critical Load is Computed for a Typical Slender PC Column

For this case of zero eccentricity, the required *EI* given by Eq. (22a) is EI_{tan} computed as follows:

(a) From Eq. (28), the strain at maximum stress of concrete, ε_0, is calculated to be:

$$\varepsilon_0 = 0.001648 + 0.0001146 \times 6$$

Table B1. Sample data for a typical column from Examples 1 to 5.

	From sectional analysis				Slender column L/r = 100	
	Eq. (15)	Eq. (14)	Eq. (18)	Eq. (19)	$P_B e$	Eq. (23)
c	M_n	P_n	EI/E_cI_g	e/h	M_B	P_B
–	0.00	314.61	–	0.00	0.00	215.32
8.00	255.18	225.47	0.486	0.14	114.21	100.91
7.49	284.40	209.18	0.507	0.17	120.53	88.65
7.31	292.82	203.74	0.510	0.18	121.97	84.86
7.14	300.58	198.28	0.512	0.19	123.08	81.19
6.97	307.67	192.82	0.511	0.20	126.06	79.00
5.77	338.97	154.20	0.466	0.27	139.71	63.56
5.09	342.56	131.75	0.415	0.33	140.36	53.98
4.91	341.85	126.08	0.400	0.34	139.84	51.57
4.74	340.51	120.38	0.385	0.35	139.11	49.18
3.89	324.31	91.35	0.300	0.44	132.31	37.27
3.71	319.18	85.43	0.283	0.47	130.44	34.91
3.54	313.41	79.45	0.265	0.49	128.46	32.57
3.03	292.13	61.28	0.211	0.60	122.16	25.63
2.86	283.61	55.16	0.193	0.64	120.06	23.35
2.69	274.30	49.02	0.176	0.70	117.93	21.08
2.00	228.90	25.06	0.109	1.14	112.06	12.27
1.31	164.77	0.09	0.052	99.00	164.77	0.00

$$= 2.332 \times 10^{-3}$$

(b) Substituting the values of L, r and ε_0 into Eq. (30), the strain at critical load, ε, is found to be:

$$\varepsilon = \left[2.332\times10^{-3} + \left(\frac{\pi \times 2.31}{231}\right)^2\right] - \sqrt{(2.332\times10^{-3})^2 + \left(\frac{\pi \times 2.31}{231}\right)^4}$$

$$= 786.7 \times 10^{-6}$$

(c) Substituting the values of ε, ε_0, and f'_c into Eq. (27), gives the value of the tangent modulus of elasticity of concrete, E_{tc}, at concentric critical load:

$$E_{tc} = \frac{2\times6}{2.33\times10^{-3}}\left(1 - \frac{786\times10^{-6}}{2.33\times10^{-3}}\right)$$

$$= 3410 \text{ ksi } (23.5 \text{ GPa})$$

(d) Substituting the values of $E_{tc,}$ and the moment of inertia of the cross section, I_g, into Eq. (21), gives the flexural rigidity, *EI*, as:

$$EI_{tan} = E_{tc} \times I_g$$
$$= 3410 \times 8^4/12$$
$$= 1163855.7 \text{ kip-in.}^2 \text{ (3341 kN-m}^2\text{)}$$

(e) The required concentric critical load, P_{cr}, is obtained by substituting the values of *EI* and L into Eq. (2), that is:

$$P_{cr} = \frac{\pi^2 \times 1163855.7}{231^2}$$

$$= 215.3 \text{ kips } (958 \text{ kN})$$

EXAMPLE 2: Shows How the Maximum Flexural Rigidity, EI_{peak}, is Obtained for a Typical PC Column Section

(a) Using Eq. (20) and substituting for the value of h = 8 in., and β_1 = 0.75, gives:

$$c_{peak} = \frac{2\times8}{3\times0.75}$$

$$= 7.11 \text{ in. } (181 \text{ mm})$$

(b) For c = 7.11 in., the nominal moment and axial load (M_n and P_n) associated with c_{peak} are given by Eqs. (14) and (15) leading to M_n = 302 kip-in., P_n =

197.3 kips.

(c) From Eq. (18), the maximum flexural rigidity is:

$$EI_{peak} = \frac{302 \times 7.11}{0.003}$$
$$= 715,740 \text{ kip - in.}^2 \ (2054 \text{ kN - m}^2)$$

(d) The corresponding eccentricity is given by Eq. (19) as:

$$e_{peak} = 302/197.3$$
$$= 1.53 \text{ in. (39 mm)}$$

EXAMPLE 3: Checking the Adequacy of Column Strength (Case 1)

Assume that the above column is subjected to a loading represented by Point A in Fig. 6 with P_A = 85 kips and M_A = 116 kip-in. Using the proposed method, compute the moment at Point A1 and check if the column can carry the loading.

(a) Compute the eccentricity for the given loading:

$$e_a = 116/85$$
$$= 1.365 \text{ in. (35 mm)}$$

(b) Because the applied eccentricity is lower than e_{peak}, use the linear *EI* relationship given by Eq. (22a):

$$EI = 1163856 - \left(\frac{1163856 - 715740}{1.53}\right) \times 1.365$$

$$= 764{,}066 \text{ kip-in.}^2 \ (2193 \text{ kN-m}^2)$$

(c) Based on the computed value of *EI*, the critical load at this eccentricity is calculated by Eq. (2):

$$P_{cr} = \frac{\pi^2 \times 764066}{231^2}$$
$$= 141.3 \text{ kips (629 kN)}$$

(d) The magnified moment is given by Eq. (10):

$$M_{A1} = \frac{116}{1 - \frac{85}{141.3}}$$
$$= 291 \text{ kip - in. (32.9 kN - m)}$$

This moment is less than the sectional moment of 319 kip-in. at a load of 85 kips, indicating that the column can indeed carry the applied load.

EXAMPLE 4: Checking the Adequacy of Column Strength (Case 2)

Assume that the above column is subjected to a loading represented by Point A in Fig. 6 with P_A = 55 kips and M_A = 149 kip-in. Using the proposed method, compute the moment at Point A1 and check if the column can carry the load.

(a) Compute the eccentricity of the given loading:

$$e_a = 149/55$$
$$= 2.71 \text{ in. (69 mm)}$$

(b) Because the eccentricity of the loading is higher than the peak eccentricity, the flexural rigidity is obtained from Eq. (22b). For such an eccentricity, sectional analysis provided M_n = 341.85 kip-in. and P_n = 126.08 kips, at a neutral axis, c = 4.91 in. Thus, Eq. (22b), gives:

$$EI = \frac{341.85 \times 4.91}{0.003}$$
$$= 559,495 \text{ kip - in.}^2 \ (1606 \text{ kN - m}^2)$$

(c) The critical load at this eccentricity is given by Eq. (2):

$$P_{cr} = \frac{\pi^2 \times 559495}{231^2}$$
$$= 103.5 \text{ kips (460 kN)}$$

(d) The magnified moment is given by Eq. (10):

$$M_{A1} = \frac{149}{1 - \frac{55}{103.5}}$$
$$= 318 \text{ kip - in. (35.9 kN - m)}$$

This moment is outside the section interaction diagram; hence, the column is not capable of carrying this load.

EXAMPLE 5: Development of a Typical Point on the Interaction Diagram

For the above column, locate Point B in Fig. 6 on the slender interaction diagram given Point D with M_D = 341.85 kip-in. and P_D = 126.08 kips as shown in Table B1.

(a) The eccentricity for this loading is e = 341.85/126.08 = 2.71 in.; it is higher than the eccentricity at the peak (e_{peak} = 1.53 in.). Accordingly, *EI* is obtained from Eq. (22b) as illustrated in Example 4 (*EI* = 559495), and the associated critical load is P_{cr} = 103.5 kips (460 kN).

(b) The first estimate of the load is obtained by using Eq. (23):

$$P_B = \frac{103.5}{1 + \frac{103.5 \times 2.71}{341.85}}$$
$$= 56.85 \text{ kips (253 kN)}$$

(c) The second estimate is obtained by substituting the moment from the sectional interaction diagram that corresponds to the axial load P_B = 56.85 kips, which is determined in this case by interpolation leading to 286.0 kip-in. Solving Eq. (23) yields:

$$P_B = \frac{103.5}{1 + \frac{103.5 \times 2.71}{286.0}}$$
$$= 52.25 \text{ kips (232 kN)}$$

(d) Step (c) may be repeated until the variation in P_B is of negligible magnitude. The correct answer for this case is P_B = 51.57 kips, which is close to the second trial shown in Step (c).

(e) The corresponding moment for the slender column is $M_B = 51.57 \times 2.71 = 139.7$ kip-in. (15.8 kN-m).

APPENDIX C — NOTATION

A_c = cross-sectional area (sq in.)
A_p = cross-sectional area of prestressing steel (sq in.)
A_g = area of gross cross section (sq in.)
b = width of rectangular cross section (in.)
c = neutral axis depth measured from compressive face of section (in.)
C_c = concrete compressive resultant force (kips)
c_{peak} = neutral axis depth that gives maximum sectional *EI* (in.)
d_{pi} = depth of steel layer, i, from compression face of section (in.)
E = modulus of elasticity (ksi)
E_c = modulus of elasticity of concrete (ksi)
EI_{peak} = maximum flexural rigidity from sectional analysis (kip-in.^{2})
EI_{tan} = tangent flexural rigidity of slender column under concentric loading (kip-in.^{2})
e_{peak} = eccentricity at which sectional flexural rigidity becomes maximum (in.)
E_s = modulus of elasticity of reinforcing bar (ksi)
E_{sc} = secant modulus of concrete (ksi)
E_{sp} = secant modulus of prestressing steel (ksi)
E_{tc} = tangent modulus of concrete (ksi)
E_{tp} = tangent modulus of prestressing steel (ksi)
f'_c = specified compressive strength of concrete (ksi)
f_{pi} = prestressing steel stress in typical layer (ksi)
F_{pi} = prestressing steel force in typical layer (kips)
h = height of rectangular cross section (in.)
I = moment of inertia of column cross section (in.^{4})
I_c = moment of inertia of cross-sectional area of concrete (in.^{4})
I_p = moment of inertia of cross-sectional area of prestressing steel (in.^{4})
I_g = gross moment of inertia of column cross section (in.^{4})
I_{se} = second moment of area of reinforcing bars in section (in.^{4})
L = column length (in.)
M_0 = nominal flexural moment capacity of the section at zero axial load (kip-in.)

M_{end}